Available online at www.sciencedirect.com
ScienceDirect
Journal of the European Ceramic Society 30 (2010) 1887–1896
www.elsevier.com/locate/jeurceramsoc

Blue-violet ceramic pigments based on Co and Mg $Co_{2-x}Mg_xP_2O_7$ diphosphates

M. Llusar [a,*], A. Zielinska [b], M.A. Tena [a], J.A. Badenes [a], G. Monrós [a]

[a] *Departamento de Química Inorgánica y Orgánica, Universitat Jaume I, 12071, Castellón, Spain*
[b] *Faculty of Chemistry, University of Wroclaw, Poland*

Received 20 November 2009; received in revised form 26 February 2010; accepted 21 March 2010

Abstract

Solid solutions of Co and Mg diphosphates with compositions $Co_{2-x}Mg_xP_2O_7$ ($x = 0$, 0.1, 0.2, 0.3, 0.5, 0.7, 1.0, 1.5 and 1.8) have been prepared and characterized for the first time as alternative low-toxicity blue ceramic pigments. The compositions were prepared through the conventional coprecipitation route and calcined up to 1000 °C/2 h. Samples were characterized by thermal analysis, XRD, SEM/EDX, UV–vis-NIR spectroscopy and colour measurements (CIE-$L^*a^*b^*$). Isostructural $Co_{2-x}Mg_xP_2O_7$ diphosphate solid solutions (monoclinic system and $P21/c$ spatial group) formed successfully within the studied range of compositions, accompanied only by a minor quantity of residual Co or Mg orthophosphates ($M_3(PO_4)_2$). Interestingly, the obtained solid solutions developed nice blue-violet colourations even with high Mg doping after enamelling within double-firing ($x = 1.5$–1.8) and single-firing ($x = 1.0$–1.5) ceramic glasses. These optimal compositions containing a minimized Co amount (measured values around 7–16 wt%) could be therefore less toxic alternatives to the conventional $Co_3(PO_4)_2$ blue ceramic pigment.

Keywords: A. Sol–gel processes; C. Colour; C. Optical Properties; Phosphates; Blue ceramic pigments

1. Introduction

Materials based on metallic phosphates are being profusely investigated due to the versatility of their structures and compositions which make these materials very suitable for many advanced applications, such as catalysts,[1,2] dielectrics, pigments,[3–6] thermo-resistant materials, molecular sieves,[7,8] sensors, photoluminescence,[9] electrochemistry,[10–12] magnetic[13,14] and biocompatible materials,[15] and so on.

Within the field of ceramic materials, some research on phosphates is directed to the development of ceramic pigments (or dyes) and also to obtain new photo-luminescent materials.[9] At present there are only two phosphate-based ceramic pigments according to the DCMA classification[16]: the violet Co phosphate ($Co_3(PO_4)_2$, DCMA 8-11-1) and Co–Li phosphate ($LiCoPO_4$, DCMA 8-12-1) pigments. Metallophosphates exhibit a great capacity for the formation of diverse solid solutions through the acceptance of different metal substitutions in the phosphate lattice. Taking advantage of this, Onoda et al. have recently synthesized ceramic pigments based on different phosphates (ortho-, di- and cyclo-tetra-phosphates) containing transition metals (i.e. Co and Ni) and also La and other rare earths (Nd) as doping ions.[3,4,17,18]

With the aim of obtaining new low-toxicity ceramic pigments,[19–22] we have recently investigated some phosphate-based pigments.[5,6] In these previous works, violet-blue ceramic pigments were prepared through the coprecipitation route in the solid solution system of Fe ($FePO_4$) and Co ($Co_3(PO_4)_2$) phosphates,[5] and also in the system of Fe and Co oxy-phosphates ($CoFeOPO_4$).[6] Through the minimization of the Co amount introduced in these solid solutions (10–20 wt%) it was possible to develop bluish ceramic pigments or dyes involving lower toxicity, similarly to previous minimization studies performed in other oxide-based Co-containing ceramic pigments (with olivine –Co_2SiO_4–, spinel –$CoAl_2O_4$–, or Co-doped willemite –$(Co,Zn)_2SiO_4$– structures).[19,23]

Taking into account these previous investigations, the aim of the present study is to develop and characterize for the first time

* Corresponding author at: Departamento de Química Inorgánica y Orgánica, Universitat Jaume I, Edifici Científico-Tècnic, Av. Sos Baynat s/n, 12071, Castellón, Spain. Tel.: +34 964 728244; fax: +34 964 728214.
E-mail address: mllusar@qio.uji.es (M. Llusar).

0955-2219/$ – see front matter © 2010 Elsevier Ltd. All rights reserved.
doi:10.1016/j.jeurceramsoc.2010.03.017

alternative blue-violet ceramic pigments based on Mg-doped Co diphosphates, $Co_{2-x}Mg_xP_2O_7$, and to minimize the Co content in these pigments. In these formulations the Co:P ratio is lower than in the conventional $Co_3(PO_4)_2$ blue pigment and, on the other hand, there is presumably a large interval of solid solution formation between the isostructural $Co_2P_2O_7$ and $Mg_2P_2O_7$ diphosphates, since both structures crystallize in the same monoclinic spatial group ($P21/c$). Therefore, through the doping with increasing amounts of Mg we could minimize to a large extent the Co content in the formulation, which may lead to an important reduction of the toxicity of the obtained blue-violet ceramic pigments.

2. Experimental procedure

2.1. Sample preparation

Solid solutions of Co and Mg diphosphates with compositions $Co_{2-x}Mg_xP_2O_7$ ($x = 0$, 0.1, 0.2, 0.3, 0.5, 0.7, 1.0, 1.5 and 1.8) were prepared through the conventional coprecipitation route, using $Co(NO_3)_2{\cdot}6H_2O$ (98%, Fluka), $Mg(NO_3)_2{\cdot}6H_2O$ (99%, Aldrich) and H_3PO_4 (80%, Fluka) as precursors. In a typical preparation of the compositions, Mg and Co salts were added (in this order) to an aqueous solution (150 mL) containing the required stoichiometric amount of H_3PO_4 (continuously stirred and at room temperature). Aqueous ammonia (NH_3:H_2O = 1:1) was then added dropwise to the homogeneous solution until reaching a pH of *ca.* 7–8. The obtained coprecipitate powders were then dried overnight in an electrical dryer, and the resulting dried powders were subsequently submitted to calcination in an electrical furnace up to 1000 °C (5 °C/min of heating gradient and 2 h of soaking time at the maximum temperature).

2.2. Sample characterization

Simultaneous differential thermal and thermogravimetric analysis (DTA-TGA) of dried coprecipitates was carried out with a Mettler Toledo thermal analyzer (using Pt crucibles with a constant 5 °C/min heating from 25 up to 1250 °C). Crystallochemical characterization of calcined samples was performed by X-ray diffraction (XRD) in a Siemens D-500 powder diffractometer with Ni-filtered CuK_α radiation (from 15° to 70° 2θ, with steps of 0.02° 2θ and a counting time of 2 s per step). A structure profile refinement was also carried out using the TOPAS program[24,25] for the semi-quantitative analysis of the present crystalline phases (wt%) and calculation of structural parameters. With this aim, much slower XRD runs were conducted from 10° to 80° 2θ, with a step size of 0.03° 2θ and a counting time of 10 s per step. The accuracy of the refinements

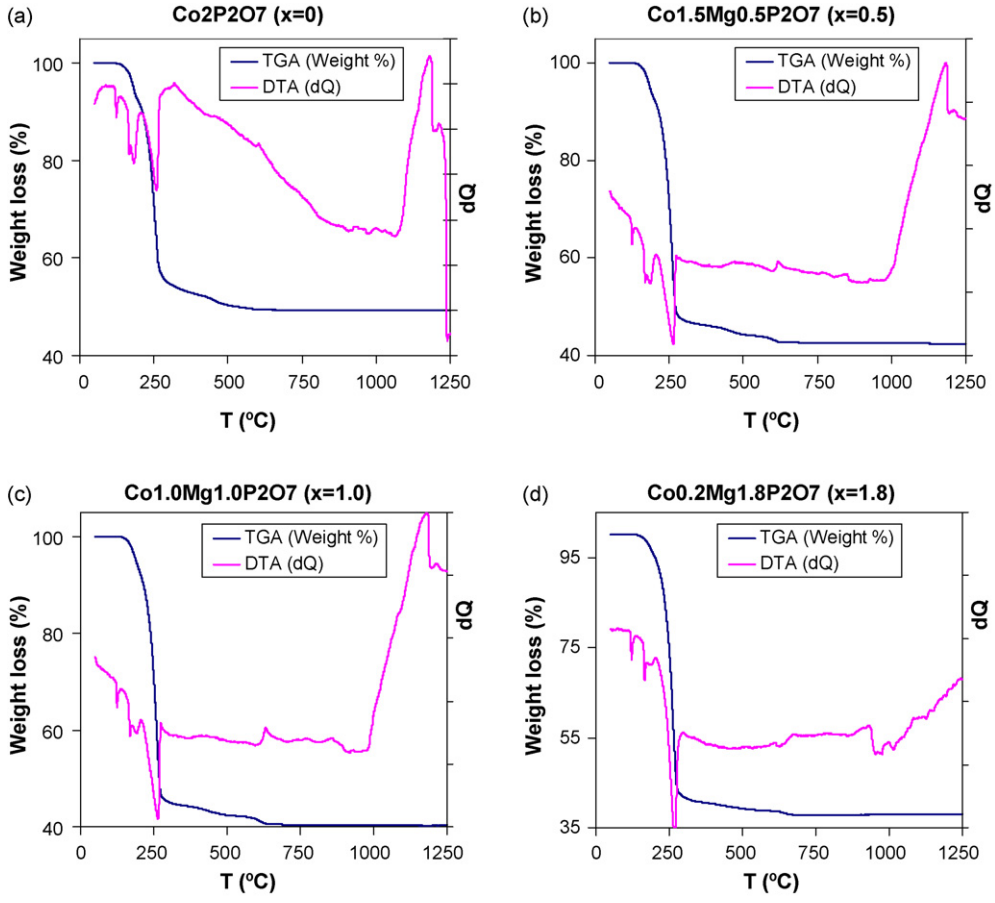

Fig. 1. Thermogravimetric (TGA) and differential thermal analysis (DTA) of representative coprecipitate $Co_{2-x}Mg_xP_2O_7$ samples: (a) $x = 0$, (b) $x = 0.5$, (c) $x = 1.0$ and (d) $x = 1.8$.

was controlled by the values of the R_{wp} ("R-weighted pattern") and GOF ("Goodness of fit") fit indicators.[26]

On the other hand, the morphology and microstructure of $Co_{2-x}Mg_xP_2O_7$ solid solutions obtained after calcination was examined by scanning electron microscopy (SEM) with a Leo-440i Leica electron microscope (as grain amounts following conventional preparation and imaging techniques). The composition and chemical homogeneity of the samples (Co:Mg:P ratio) was determined by semi-quantitative elemental analysis with an EDX analyzer (supplied by Oxford University) attached to the microscope.

In order to test the performance of the obtained solid solutions as blue-violet ceramic pigments, the powders calcined at 1000 °C were 5 wt% enamelled within commercial double-firing and single-firing transparent glasses (SiO_2–CaO–ZnO system) onto conventional ceramic biscuits, and fired following a fast-firing scheme (52 min of duration from cool to cool at a maximum temperature of 1050 °C for the double-firing glass, and 1080 °C for the single-firing glass). The optical properties of enamelled samples were then analyzed by diffuse reflectance spectroscopy (UV–vis-NIR) performed with a Perkin-Elmer (lambda 2000) spectrophotometer. In addition, $L^*a^*b^*$ colour parameters of enamelled samples (with both glasses) were measured using a standard lighting C, following the CIE-$L^*a^*b^*$ colorimetric method recommended by the CIE (Commission Internationale de l'Eclairage).[27] On this method, L^* is the lightness axis (black (0) → white (100)), b^* is the blue (−) → yellow (+) axis, and a^* is the green (−) → red (+) axis.

3. Results and discussion

3.1. Thermal analysis (DTA–TGA)

The differential thermal (DTA) and thermogravimetric (TGA) analyses of representative $Co_{2-x}Mg_xP_2O_7$ coprecipitate powders are shown in Fig. 1. In all samples three endothermic peaks around 125, 180 and 265 °C can be first observed in the DTA curves, all of them accompanied by an important weight loss (above 50 wt%) in the TGA curves. These peaks and the associated weight loss correspond to the elimination of water and to the decomposition of the NH_4NO_3 present in the coprecipitate powders. Moreover, a small weight loss (around 4–6%) is also observed in all samples extending from *ca.* 330 °C until 650–700 °C. This weight loss could be presumably associated to the condensation of $H_xPO_4^{3-x}$ into diphosphate $P_2O_7^{4-}$ species, with the consequent H_2O elimination. Also noticeable, an intense exothermic signal is observed at higher temperatures (from 980 to 1080 °C up to 1187 °C) in all DTA curves for $x \leq 1.0$. This exothermic effect would correspond to the crystallization of $Co_{2-x}Mg_xP_2O_7$ diphosphates. Noteworthy, in the case of Mg-enriched samples with nominal compositions $x = 1.5$ (not shown) and $x = 1.8$ (Fig. 1d), this exothermic effect is clearly less intense and also shifted to higher temperatures (the maximum is at 1233 °C for $x = 1.5$ and is higher than 1250 °C for $x = 1.8$). These samples correspond to $Mg_2P_2O_7$ diphosphates doped with very small quantities of Co ($Co_{0.5}Mg_{1.5}P_2O_7$ and $Co_{0.2}Mg_{1.8}P_2O_7$, respectively), and thus its crystallization appears to be different (less exothermic and at higher temperatures) to that of samples more Co-enriched ($x \leq 1.0$). Interestingly, for $x = 0$ this exothermic band is subsequently followed by an endothermic band starting at 1206 °C and with the peak centred at around 1242 °C, which is associated to the melting of the cobalt diphosphate ($Co_2P_2O_7$). This melting point is also progressively shifted to higher temperatures (above 1250 °C) with the increase of Mg doping (x) in the solid solution, being this effect more evident for samples with $x = 1.5$ (not shown) and $x = 1.8$ (the melting point of $Mg_2P_2O_7$ is 1395 °C).

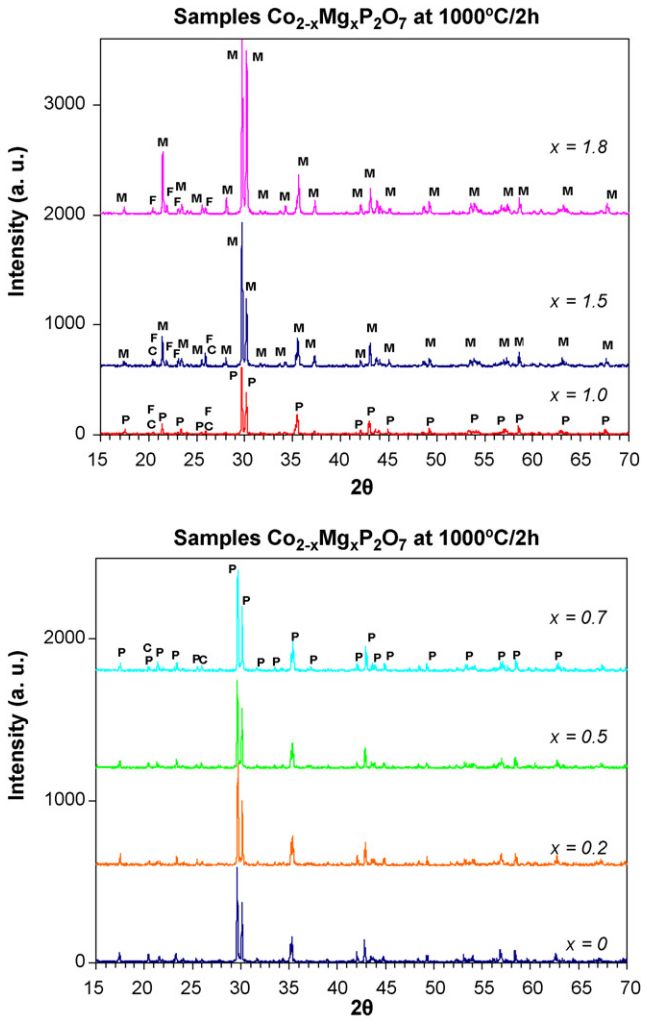

Fig. 2. XRD patterns of representative coprecipitate $Co_{2-x}Mg_xP_2O_7$ samples fired at 1000 °C/2 h. Crystalline phases: P, $Co_2P_2O_7$; M, α-$Mg_2P_2O_7$; C, $Co_3(PO_4)_2$; F, $Mg_3(PO_4)_2$ (farringtonite).

3.2. X-ray diffraction characterization (XRD)

The XRD patterns of representative $Co_{2-x}Mg_xP_2O_7$ compositions fired at 1000 °C/2 h are shown in Fig. 2. Remarkably, the isostructural Mg-doped Co diphosphate ($Co_2P_2O_7$; PDF number 01-084-2126, labelled as P in Fig. 2) or Co-doped Mg diphosphate (α-$Mg_2P_2O_7$; PDF number 01-072-0019, labelled as M in Fig. 2) formed as the major crystalline phases in all samples.

Table 1
Results of the refinement (with the TOPAS program)[24] of XRD patterns for representative $Co_{2-x}Mg_xP_2O_7$ powdered samples (1000 °C-fired).

Sample	Refinement fit indicators[a]		Crystalline phases (wt%) (Rietveld)	Cell parameters and cell volume of the $(Co,Mg)_2P_2O_7$ major phase				
	R_{wp}	GOF		*a*	*b*	*c*	*β*	Volume
$x=0.0$	16.23	1.20	$(Co,Mg)_2P_2O_7$ (95.1 ± 2) $Co_3(PO_4)_2$ (4.9 ± 2)	7.0061 (1)	8.3635 (1)	9.0111 (2)	113.652 (1)	483.65 (2)
$x=0.2$	16.17	1.22	$(Co,Mg)_2P_2O_7$ (95.8 ± 3) $Co_3(PO_4)_2$ (4.2 ± 3)	6.9996 (1)	8.3548 (2)	9.0153 (2)	113.668 (1)	482.88 (2)
$x=0.5$	16.46	1.27	$(Co,Mg)_2P_2O_7$ (93.6 ± 2) $Co_3(PO_4)_2$ (6.4 ± 2)	6.9919 (1)	8.3448 (2)	9.0239 (2)	113.695 (1)	482.12 (2)
$x=1.0$	15.59	1.26	$(Co,Mg)_2P_2O_7$ (95.3 ± 4) $Co_3(PO_4)_2$ (3.3 ± 3) $Mg_3(PO_4)_2$ (1.4 ± 3)	6.9766 (1)	8.3266 (2)	9.0348 (2)	113.744 (1)	480.42 (2)
$x=1.5$	15.17	1.35	$(Co,Mg)_2P_2O_7$ (90.7 ± 4) $Co_3(PO_4)_2$ (4.9 ± 3) $Mg_3(PO_4)_2$ (4.4 ± 4)	6.9612 (2)	8.3082 (2)	9.0436 (3)	113.798 (1)	478.56 (2)
$x=1.8$	15.48	1.54	$(Co,Mg)_2P_2O_7$ (93.8 ± 2) $Mg_3(PO_4)_2$ (6.2 ± 2)	6.9543 (2)	8.2996 (2)	9.0500 (2)	113.826 (1)	477.83 (2)

[a] Refinement fit indicators: R_{wp} ("R-weighted pattern") and GOF ("Goodness of fit").[26]

Effectively, the XRD peaks of Co diphosphate are observed in all samples up to composition with $x=1$ ($Co_1Mg_1P_2O_7$), while the XRD peaks of Mg diphosphate are observed in samples with $x=1.5$ ($Co_{0.5}Mg_{1.5}P_2O_7$) and $x=1.8$ ($Co_{0.2}Mg_{1.8}P_2O_7$). Both crystalline phases belong to the monoclinic system and crystallize in the *P*21/*c* (14) spatial group (the PDF file of α-$Mg_2P_2O_7$ was originally published as belonging to the *B*121/*C*1(8) spatial group, but it has been standardized to the monoclinic *P*21/c (14) spatial group in the new ICSD data base).[28] Although the XRD patterns of both compounds are very similar, they may be easily distinguished by the much increased intensity of the peaks around 21.4–21.6° 2 and around 28.1° 2 in the case of α-$Mg_2P_2O_7$. Moreover, the successful formation of the $Co_{2-x}Mg_xP_2O_7$ solid solutions was confirmed by the presence of minor intensity residual peaks of the corresponding orthophosphates, $Co_3(PO_4)_2$ for $x \leq 1.5$ (PDF number 01-070-1795 and labelled as C in Fig. 2) and $Mg_3(PO_4)_2$ (farringtonite) for $x \geq 1.0$ (PDF number 01-075-1491 and labelled as F in Fig. 2), and also by the variation of the measured cell parameters (commented below).

Table 1 summarizes the results of the refinement profile performed with the TOPAS program[24] showing the fit indicators (R_{wp} and GOF),[26] the phase content analysis (wt%) and the calculated cell parameters (and cell volume). As the first observation, the obtained values for the R_{wp} (around 15–16) and GOF (around 1.2–1.5) fit criteria are indicative of refinements with and acceptably good confidence degree.[26] Moreover, the measured phases content (wt%) in all the samples indicates that they are majorly constituted by the diphosphate solid solution (90.7–95.8 wt%), and only minor (residual) quantities of the residual Co and Mg orthophosphates are present (from 1.4 to 6.4 wt%).

On the other hand, there is also a clear linear tendency in the variation of cell parameters of the diphosphates with the composition (see also Fig. 3). In this respect, the calculated cell parameters *a* and *b* decrease linearly with increasing amounts of Mg (*x*) in the formulation, while the parameter *c* increases also linearly with Mg doping. As a result, the overall cell volume of the $(Co,Mg)_2P_2O_7$ solid solution diminishes (linearly) a little bit, which is consistent with the slightly smaller ionic size of Mg^{2+} in six-fold coordination (86 pm), with respect to the size of 6-coordinated (high spin) Co^{2+} (88.5 pm).[29]

3.3. Electron microscopy characterization (SEM/EDX)

To gain further information about the morphology, homogeneity and composition of the samples at the microscale, SEM/EDX characterization was performed with selected fired samples. SEM observations of representative $Co_{2-x}Mg_xP_2O_7$

Table 2
Theoretical (initial) formulations and the corresponding EDX-measured average compositions for selected coprecipitate samples (1000 °C-fired powders).

Sample	Theoretical formulation	Average EDX composition (atomic)[a]			
		Co	Mg	P	O
$x=0.0$	$Co_2P_2O_7$	2.3 (6)	–	2.0 (1)	7.4 (7)
$x=0.5$	$Co_{1.5}Mg_{0.5}P_2O_7$	1.7 (2)	0.5 (1)	2.0 (1)	7.1 (2)
$x=0.7$	$Co_{1.3}Mg_{0.7}P_2O_7$	1.30 (5)	0.67 (2)	2.00 (4)	7.50 (6)
$x=1.0$	$Co_1Mg_1P_2O_7$	1.0 (1)	0.95 (4)	2.00 (6)	7.1 (1)
$x=1.5$	$Co_{0.5}Mg_{1.5}P_2O_7$	0.67 (7)	1.42 (6)	2.0 (3)	7.1 (2)
$x=1.8$	$Co_{0.2}Mg_{1.8}P_2O_7$	0.25 (5)	1.54 (3)	2.0 (2)	6.4 (4)

[a] The compositions have been normalized to 2 mol of P. The standard deviation is shown between brackets.

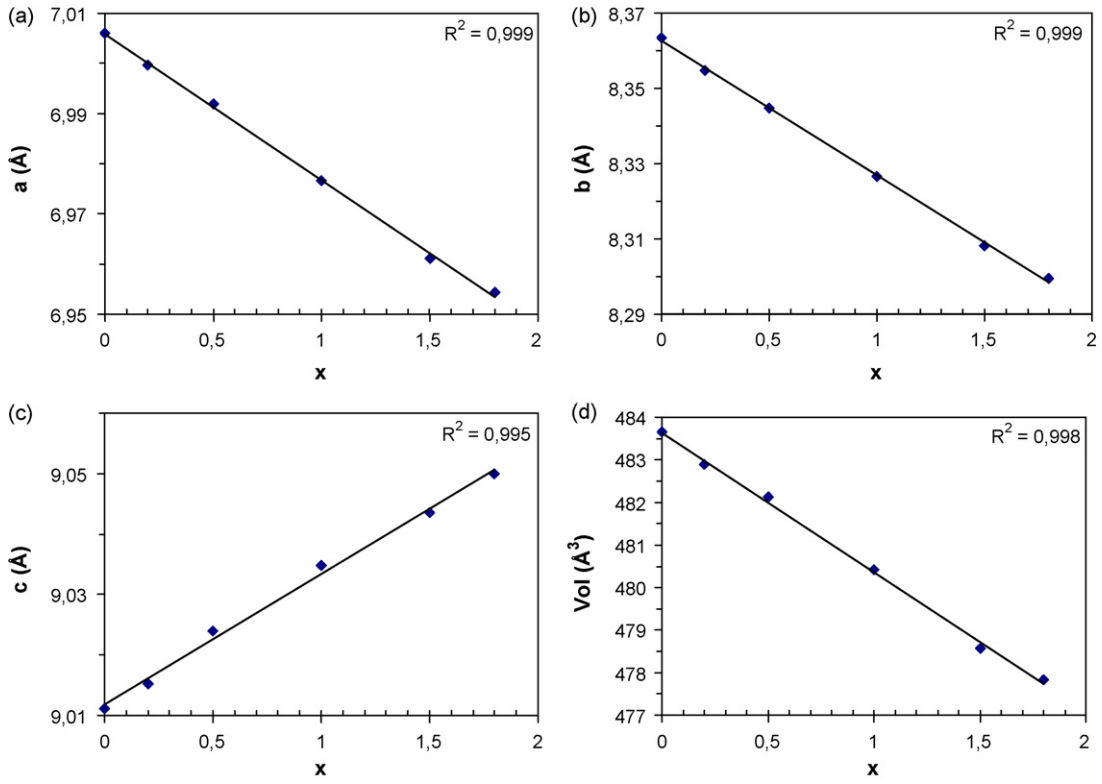

Fig. 3. Evolution of cell parameters *a*, *b* and *c* (a–c), and cell volume (d) with Mg doping (*x*) for representative diphosphate $Co_{2-x}Mg_xP_2O_7$ samples ($x = 0$, 0.2, 0.5, 1.0, 1.5 and 1.8) fired at 1000 °C/2 h (obtained from the TOPAS refinement profile[24]).

powders calcined at 1000 °C (see Fig. 4) let us appreciate that the samples are formed by aggregates of different sizes (around 5–50 μm) constituted by smaller particles or grains (1–3 μm) with rounded morphologies, and partially sintered. In general terms, the morphology is quite homogeneous and there are not considerable differences in the brightness or contrast signal throughout the samples. This is indicative of quite an homogeneous composition of the samples throughout the different aggregates or grains (the images were obtained with the electron backscattering detector; except for $x = 0$).

To characterize in a semi-quantitative way the chemical composition and homogeneity of the samples, EDX analyses were performed in different regions of the samples. Representative EDX analyses of selected samples ($x = 0$, 0.5, 1.0 and 1.5) are shown in Fig. 5. The analyses showed that the samples were quite homogeneous, obtaining only a slight dispersion in the molar Co:Mg:P ratios through the different analyzed regions. The theoretical and experimental (EDX-measured) average compositions of selected samples (semi-quantitative values) are summarized in Table 2. As it may be observed the experimental average compositions are quite close to the theoretical initial formulations (considering the standard deviation). In some cases a small deviation from the theoretical stoichiometry is observed, which can be due to a non-sufficiently homogeneous or complete precipitation of the metal species from the liquid phase in the preparation of precursor samples. A representative EDX mapping analysis of sample with $x = 1.0$ ($CoMgP_2O_7$) is provided in Fig. 6, confirming the homogenous (even) distribution of all elements (Co, Mg and P) through the sample. The narrow variability of the chemical composition in this sample may be also visualized in the triangular composition diagram included in this figure (bottom, left; obtained with the EDX analyses of multiple points of the analyzed region).

3.4. UV–vis-NIR spectroscopy and colour characterization

Fig. 7 shows the UV–vis-NIR spectra of representative diphosphate $Co_{2-x}Mg_xP_2O_7$ powders fired at 1000 °C/2 h. A multiple band around 500 nm (472, 525 and 591 peaks), along with other three bands centred at around 850, 1238 and 1683 nm may be observed in all powdered samples. These bands are in good accordance with the presence of Co^{2+} ions in both octahedral and trigonal bipyramidal coordination, which are the two crystallographic sites for the cobalt ion in the diphosphate ($Co_2P_2O_7$) and orthophosphate ($Co_3(PO_4)_2$) structures.[30,31] In effect, the bands around 1238, 591 and 525 can be assigned to ν_1 ($^4T_1$ (F) → $^4T_2$ (F)), ν_2 ($^4T_1$ (F) → $^4A_2$ (F)), and ν_3 ($^4T_1$ (F) → $^4T_1$ (P)) spin-allowed transitions of Co^{2+} ions in an octahedral ligand field, respectively.[23] On the other hand, the bands around 1683, 850 and 472 nm could correspond to $^4A_2 \rightarrow {}^4A_1$ (2500–1111 nm), $^4A_2 \rightarrow {}^4E$ (1000–676 nm) and $^4A_2 \rightarrow {}^4E$ (P) (582–476 nm) transitions of Co^{2+} in high spin trigonal bipyramidal sites.[5] In these sites, the transitions from the $^4A_2$ ground state generally occur both in the near infrared and in the visible region, and the spectra of these species are quite rich.[32]

Interestingly, after enamelling the fired powders in both double-firing and single-firing glasses, the UV–vis-NIR spectra present distinct features (see Fig. 8), with a very broad band

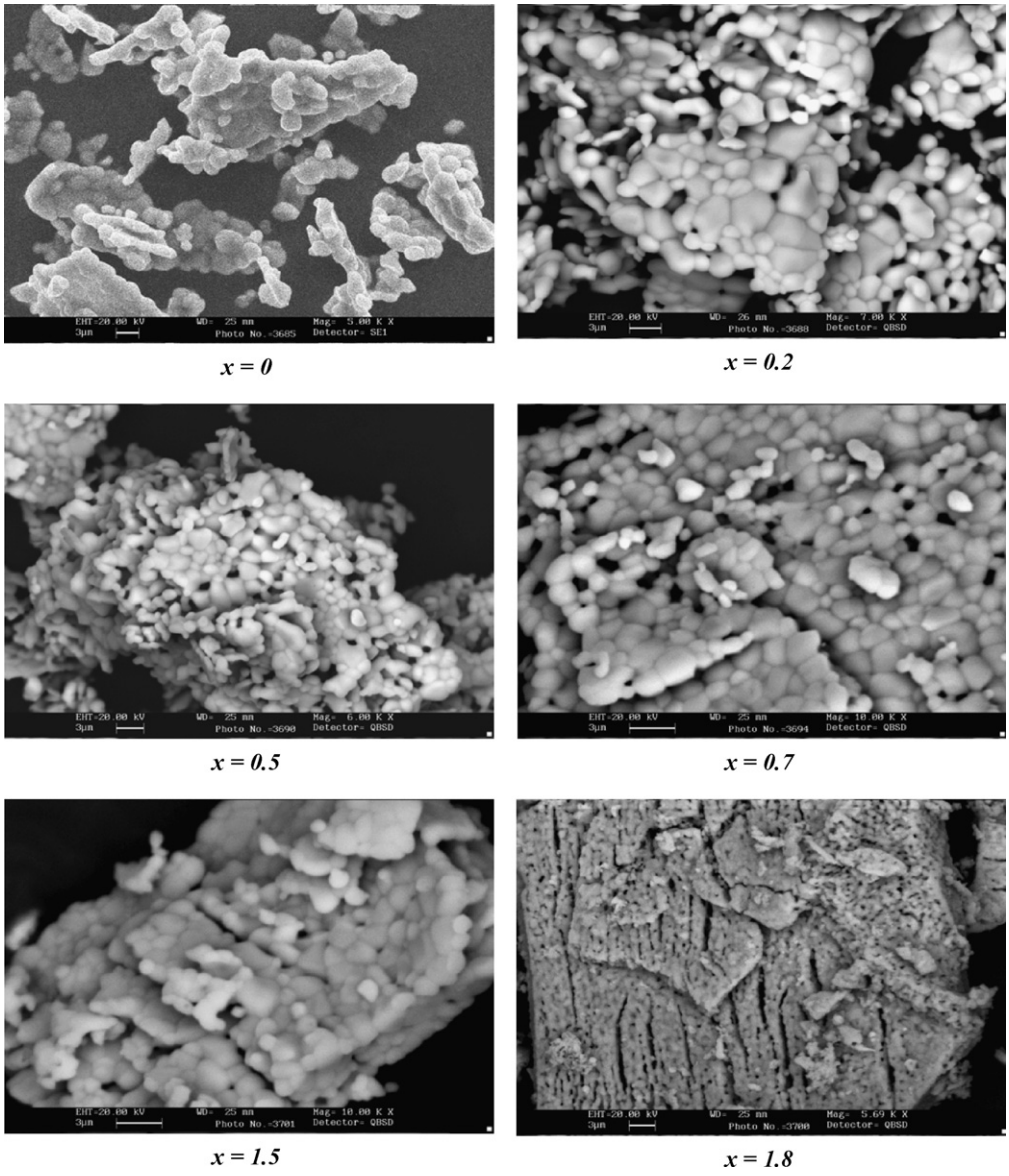

Fig. 4. SEM images of representative $Co_{2-x}Mg_xP_2O_7$ samples fired at 1000 °C/2 h. The images have been obtained with the backscattering electron detector for all samples except for $x = 0$ (secondary electron detector).

extending in the near infrared region from 1200 to 1948 nm, and a multiple band with peaks (or shoulders) centred at around 540, 600 and 650 nm. The change in the position of the bands of enamelled samples with respect to the spectra of powdered samples is indicating a change in the Co^{2+} coordination from 5 and 6 (powdered samples) to 4 (enamelled samples). Indeed, in the case of tetrahedral Co^{2+} the two first spin-allowed bands (ν_1: $^4A_2$ (F) → $^4T_2$ (F); ν_2: $^4A_2$ (F) → $^4T_1$ (F)) fall in the infrared region (around 1400 and 1600 nm), and only the third one is present in the blue region of the visible, usually as a triple band around 540, 590, and 640 nm.[19] These transitions are in agreement with the observed experimental bands. Accordingly, these results indicate that during the enamel firing the Co^{2+} ions would be diffusing from their coordination sites in the pigment ($Co_2P_2O_7$ structure) to tetrahedral sites of the glassy matrix.[5,6,23]

Regarding the performance as blue-violet ceramic pigments of the obtained diphosphate solid solutions, the colour parameters (CIE-$L^*a^*b^*$) of samples enamelled within both double-firing and single-firing glasses are summarized in Table 3. The aspect of enamelled samples is also presented in Fig. 9, in which two reference samples enamelled with the clas-

Table 3
Colour parameters (CIE-$L^*a^*b^*$) of representative $Co_{2-x}Mg_xP_2O_7$ samples (1000 °C-fired) enamelled within the double-firing and single-firing glasses.

Single-firing glass				Double-firing glass			
Sample	L^*	a^*	b^*	Sample	L^*	a^*	b^*
$x = 0$	38.4	10.1	−28.9	$x = 0$	35.8	9.2	−26.4
$x = 0.2$	39.5	10.3	−29.4	$x = 0.2$	36.4	9.0	−29.7
$x = 0.5$	40.6	10.6	−30.0	$x = 0.5$	34.9	10.5	−29.3
$x = 1.0$	45.9	10.4	−30.4	$x = 1.0$	39.6	10.0	−30.9
$x = 1.5$	58.6	7.6	−25.0	$x = 1.5$	45.0	9.3	−34.8
$x = 1.8$	70.2	4.7	−18.7	$x = 1.8$	53.0	6.0	−32.9

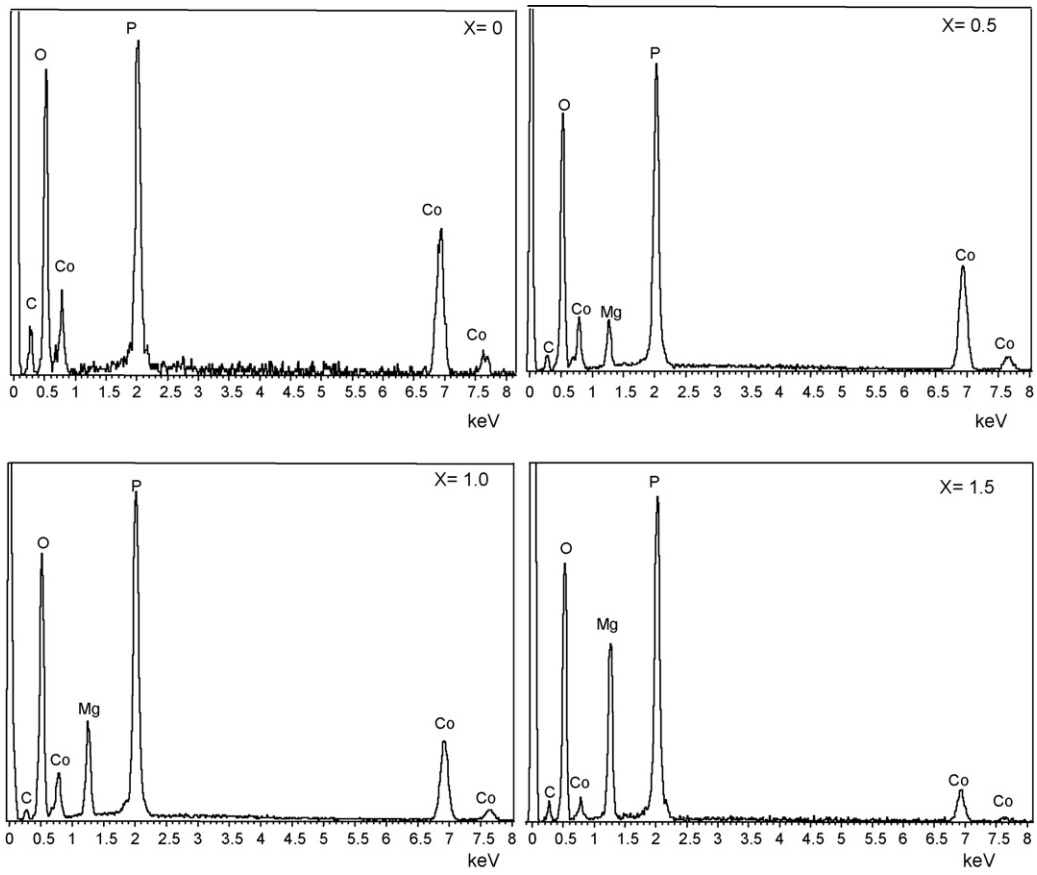

Fig. 5. Representative EDX analyses of selected $Co_{2-x}Mg_xP_2O_7$ samples.

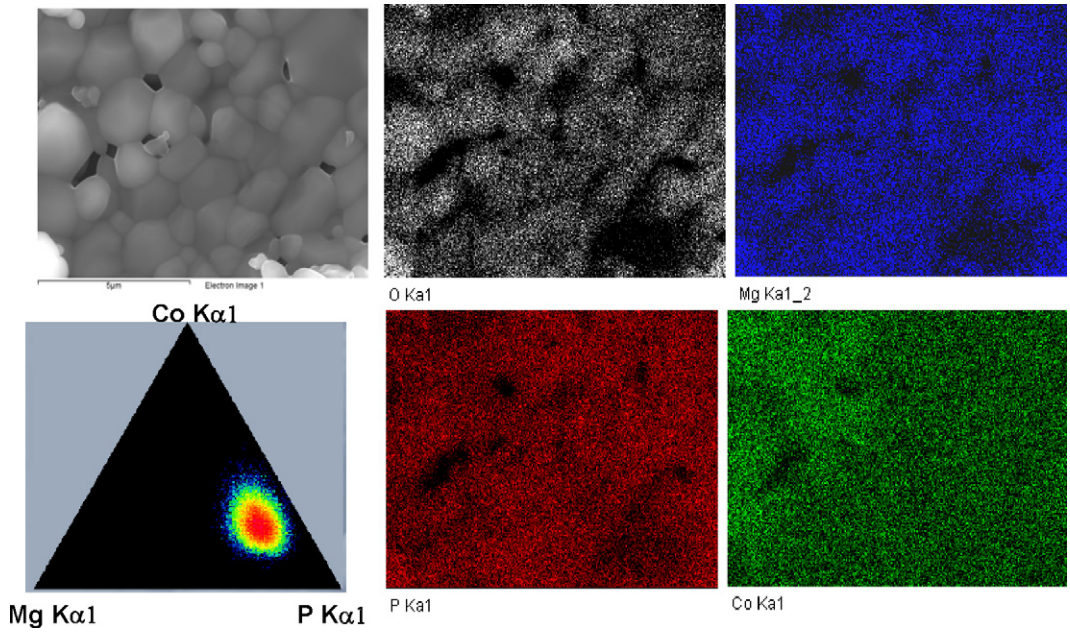

Fig. 6. Representative EDX mapping analysis of sample $Co_1Mg_1P_2O_7$ ($x = 1$). A triangular composition diagram (bottom, left) showing the composition variation through the analyzed region (up, left) is also presented.

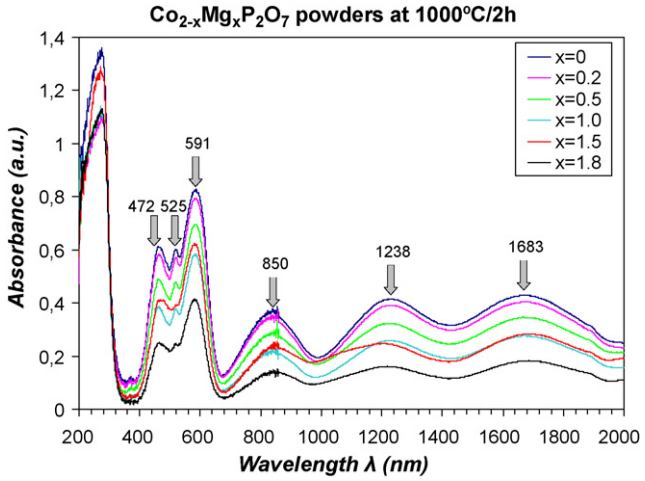

Fig. 7. UV–vis-NIR spectra corresponding to representative $Co_{2-x}Mg_xP_2O_7$ powders fired at 1000 °C/2 h. (For interpretation of the references to colour in this figure legend, the reader is referred to the web version of the article.)

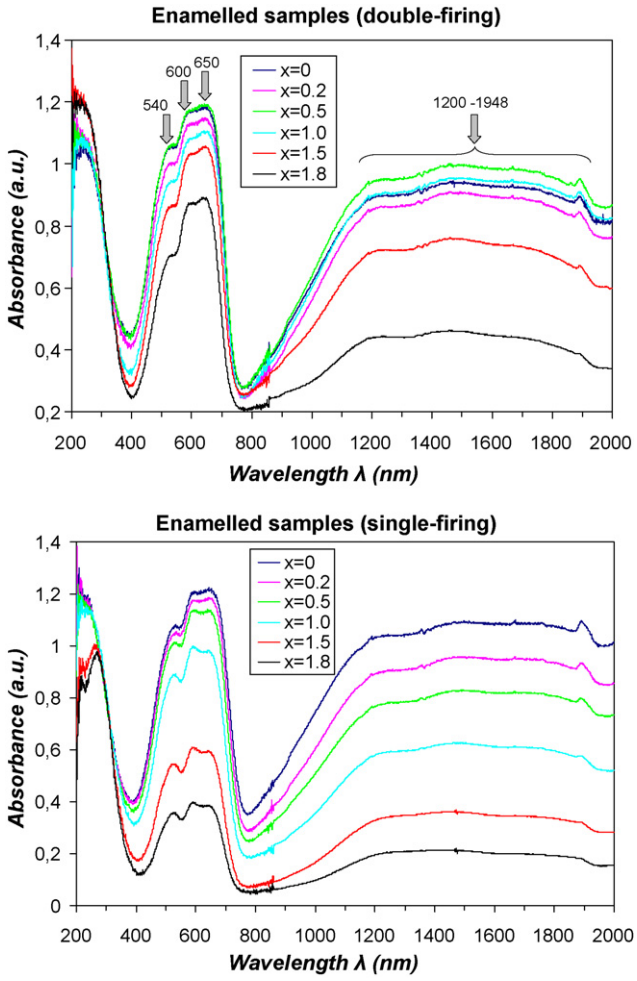

Fig. 8. UV–vis-NIR spectra corresponding to representative $Co_{2-x}Mg_xP_2O_7$ samples enamelled with the double-firing glass (above) and with the single-firing glass (below). (For interpretation of the references to colour in this figure legend, the reader is referred to the web version of the article.)

sical Co orthophosphate pigment ($Co_3(PO_4)_2$) are also shown for comparison reasons. From these results it is possible to establish the compositional range for which the suitable blue colour is maintained in both ceramic glasses.

As it may be appreciated (Table 3 and Fig. 9), in both glasses the samples present an intense blue-violet colour, even with a Mg doping as high as $x = 1.0$. The intense blue-violet colour obtained up to $x = 1.0$ in both glasses is confirmed by the large negative b^* values (from −26 to −31), which give the blue component, and by the smaller but considerable positive a^* values (between 9 and 11), which correspond to the red hue. The L^* component is quite low (values around 36–46), indicating considerably dark or intense colours. This blue-violet colour is consistent with the reflectance spectra of enamelled samples (see for instance the spectra obtained with the double-firing glass in Fig. 10), that present two intense and broad bands (reflectance) in the blue (around 400 nm) and red (around 750 nm) regions of the spectra. Remarkably, these colour parameters are quite similar to those presented by reference samples enamelled with the $Co_3(PO_4)_2$ pigment, which are only slightly darker ($L^*/a^*/b^*$ values of 35.7/9.3/−27.6 for the double-firing glass, and 37.2/11.3/−30.5 for the single-firing glass).

At a higher Mg doping (samples with nominal compositions $x = 1.5$ or $x = 1.8$), in the case of the single-firing glass the blue component diminishes considerably (−25 or −19, respectively), similarly to the red component that also decreases (8 or 5). Besides, the L^* component increases considerably (from 38–46 to 59–70), which corresponds to less intense or lighter colours. As a result, at this higher Mg doping ($x = 1.5$ or $x = 1.8$) the colour of samples enamelled with the single-firing glass is a lighter, pale violet. In comparison, and very remarkably, the samples enamelled with the double-firing glass present a much purer and relatively intense blue colour for these compositions having a maximized Mg doping ($x = 1.5$ and 1.8) or a minimized Co content (experimental average Co wt% around 16 and 7%, respectively). Indeed, these samples present a more negative b^* value (−35 and −33, respectively), and the red component (a^*) diminishes (to 6) in the case of sample with $x = 1.8$ (it is maintained to 9 for $x = 1.5$), while still presenting relatively low L^* values (45 or 53).

In conclusion, the compositional range for which the intense blue-violet colour is maintained extends up to $x = 1.0$ (experimental Co wt% around 23%) in the case of the single-firing glass and even up to $x = 1.5$ (measured Co wt% around 16%) for the double-firing glass. In this glass it is even possible to obtain an intense and pure blue colouration ($L^*/a^*/b^* = 53/6/-33$) with a maximized Mg doping (nominal composition $x = 1.8$) or minimized amount of Co (experimental Co wt% around 7%). Thus, these results confirm that intense blue-violet colours can be obtained with the synthesized Co and Mg diphosphates, and the optimal compositions (measured Co wt% around 7–16%) can be clearly less toxic alternatives to the classical $Co_3(PO_4)_2$ blue ceramic pigment. These results are also comparable to those obtained with previously studied solid solutions in the $Fe_{1-x}Co_xPO_{4-x/2}$ (12–20 wt% of Co) and $Co_{1-x}Fe_{1+x}O_{1-x}(PO_4)_{1+x}$ (10 wt%) systems.[5,6]

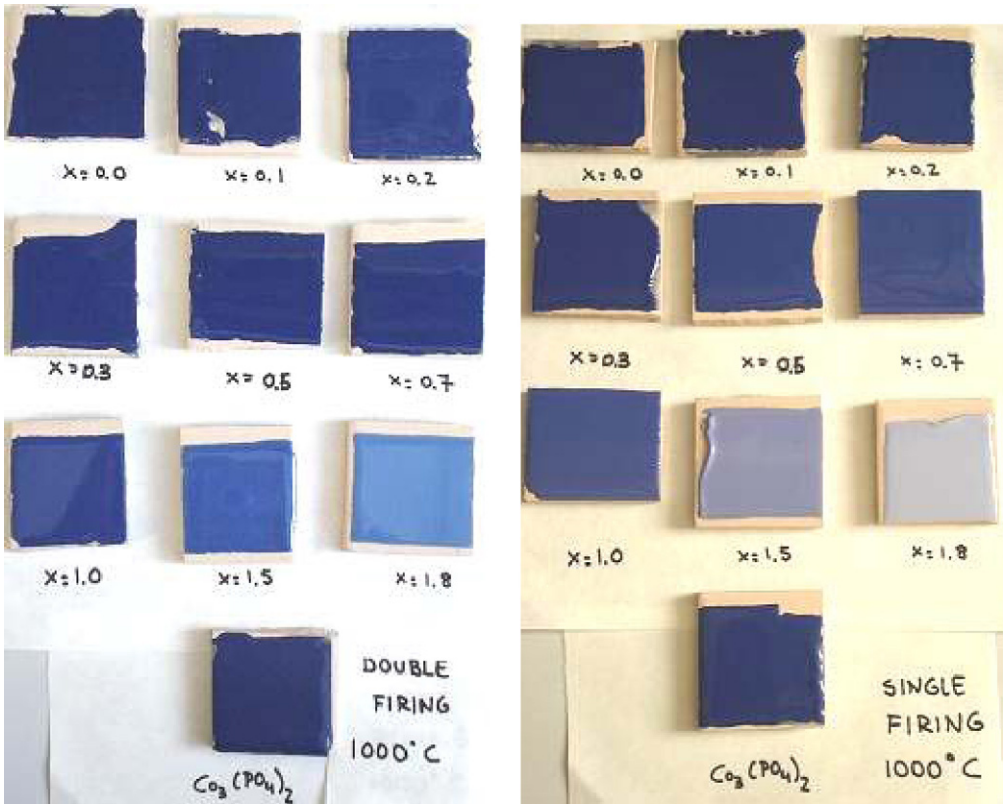

Fig. 9. Aspect of $Co_{2-x}Mg_xP_2O_7$ samples (1000 °C-fired) enamelled with the double-firing glass (left) and with the single-firing glass (right). (For interpretation of the references to colour in this figure legend, the reader is referred to the web version of the article.)

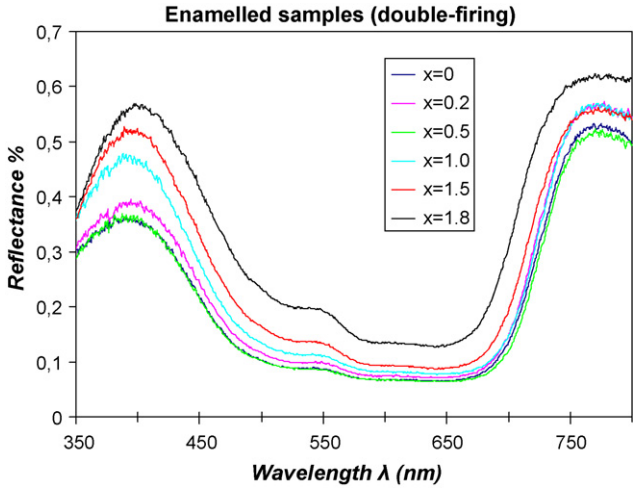

Fig. 10. Reflectance spectra corresponding to representative $Co_{2-x}Mg_xP_2O_7$ samples enamelled with the double-firing glass 1000 °C/2 h. (For interpretation of the references to colour in this figure legend, the reader is referred to the web version of the article.)

4. Conclusions

In this study we have analyzed for the first time the preparation through the coprecipitation route of alternative blue-violet ceramic pigments based on solid solutions of Co and Mg diphosphates ($Co_{2-x}Mg_xP_2O_7$). Isostructural and relatively homogeneous $Co_{2-x}Mg_xP_2O_7$ diphosphate solid solutions (monoclinic *P*21/*c* spatial group) formed successfully within the studied range of compositions (from $x = 0.2$ to $x = 1.8$), accompanied only by minor quantities of residual Co or Mg orthophosphates ($M_3(PO_4)_2$). Interestingly, through the doping with increasing amounts of Mg it was possible to minimize to a large extent the Co content in the formulation, while maintaining an acceptably blue-violet colour in the enamelled pigments, especially within the double-firing glass. Accordingly, an important reduction of the toxicity of the obtained ceramic pigments may be accomplished. The selected optimal samples with nominal compositions $x = 1.5$ and 1.8 (experimental Co wt% around 16 and 7%, respectively) could be therefore less toxic alternatives to the classical phosphate-based $Co_3(PO_4)_2$ blue ceramic pigment. These results would be comparable to those of previous Co-minimization studies performed with other phosphate-based[5,6] or oxide-based Co-containing ceramic pigments (having olivine (Co_2SiO_4), spinel ($CoAl_2O_4$), or Co-doped willemite ($(Co,Zn)_2SiO_4$) structures).[19,23]

Acknowledgements

The authors thank the Spanish "*Ministerio de Educación y Ciencia*" (Project MAT2008-02893) for financial support. Moreover, the technical assistance provided by the Central Services of Scientific Instrumentation (SCIC) of the University Jaume I is also fully acknowledged. We are also specially grateful to G. Peris (SCIC) for his technical assistance in the refinement of XRD patterns with the TOPAS program.

References

1. Onoda H, Nariai H, Moriwaki A, Motooka I. Formation and catalytic characterization of various rare earth phosphates. *J Mater Chem* 2002;**12**:1754–60.
2. Yu D, Wu C, Kong Y, Xue N, Guo X, Ding W. Structural and catalytic investigation of mesoporous iron phosphate. *J Phys Chem C* 2007;**111**:14394–9.
3. Onoda H, Yokouchi K, Kojima K, Nariai H. Addition of rare earth cation on formation and properties of various cobalt phosphates. *Mater Sci Eng B* 2005;**116**:189–95.
4. Onoda H, Matsui H, Tanaka I. Improvement of acid and base resistance of nickel phosphate pigment by the addition of lanthanum cation. *Mater Sci Eng B* 2007;**141**:28–33.
5. Meseguer S, Tena MA, Gargori C, Badenes JA, Llusar M, Monrós G. Structure and colour of cobalt ceramic pigments from phosphates. *Ceram Int* 2007;**33**:843–9.
6. Meseguer S, Tena MA, Gargori C, Galindo R, Badenes JA, Llusar M, et al. Development of blue ceramic dyes from cobalt phosphates. *Ceram Int* 2008;**34**:1431–8.
7. Pan C, Yuan S, Zhang W. A neutral templating route to mesoporous titanium phosphate molecular sieves with enhanced thermal resistance. *Appl Catal A* 2006;**312**:186–93.
8. Chandra D, Kishor N, Bhaumik A. Novel silicontinphosphate molecular sieve with high anion exchange capacity. *J Mol Catal A* 2006;**247**:216–21.
9. Buissete V, Giaume D, Gacoin T, Boilot J-P. Aqueous routes to lanthanide-doped oxide nanophosphors. *J Mater Chem* 2006;**16**:529–39.
10. Hogarth WHJ, Diniz da Costa JC, Drennan J, (Max) Lu CQ. Proton conductivity of mesoporous sol–gel zirconium phosphates for fuel cell applications. *J Mater Chem* 2005;**15**:754–8.
11. Santos-Peña J, Soudan P, Otero C, Turnes G, Franger S. Electrochemical properties of mesoporous iron phosphate in lithium batteries. *J Solid State Electrochem* 2006;**10**:1–9.
12. Song Y, Yang S, Zavalij PY, Whittingham MS. Temperature-dependent properties of $FePO_4$ cathode materials. *Mater Res Bull* 2002;**37**:1249–57.
13. Zhang X, Xu J-Q, Yu J-H, Lu J, Xu Y, Chen Y, et al. Structural characterizations and magnetic properties of three new reduced molybdenum phosphates. *J Solid State Chem* 2007;**180**:1949–56.
14. de Pedro I, Jubera V, Rojo JM, Lezama L, Sánchez J, Rodríguez J, et al. *J Magn Magn Mater* 2004;**272–276**:e665–6.
15. Vallet-Regi M. Revisiting ceramics for medical applications. *Dalton Trans* 2006:5211–20.
16. DCMA. *Classification and chemical description of the mixed metal oxide inorganic coloured pigments*. second ed. Washington, DC: Dry Color Manufacturer Association; 1982.
17. Onoda H, Nariai H, Maki H, Motooka I. Synthesis and surface properties of copper and magnesium cyclo-tetraphosphates containing rare earth elements. *Phosphor Res Bull* 2001;**12**:139–48.
18. Onoda H, Tange K, Tanaka I. Influence of lanthanum addition on preparation and powder properties of cobalt phosphates. *J Mater Sci* 2008;**43**:5483–8.
19. Fores A, Llusar M, Badenes JA, Calbo J, Tena MA, Monrós G. Cobalt minimisation in willemite ($Co_xZn_{2-x}SiO_4$) ceramic pigments. *Green Chem* 2000;**2**(3):93–100.
20. García A, Llusar M, Calbo J, Tena MA, Monrós G. Low-toxicity red ceramic pigments for porcelainised stoneware from lanthanide–ceria solid solutions. *Green Chem* 2001;**3**:238–42.
21. Jansen M, Letschert HP. Inorganic yellow-red pigments without toxic metals. *Nature* 2000;**404**:980–2.
22. Furukawa S, Masui T, Imanaka N. Synthesis of new environmentally friendly yellow pigments. *J Alloys Compd* 2006;**418**:255–8.
23. Llusar M, Forés A, Badenes JA, Calbo J, Tena MA, Monrós G. Colour analysis of some cobalt-based blue pigments. *J Eur Ceram Soc* 2001;**21**:1121–30.
24. Bruker AXS (2003): TOPAS V2.1. General profile and structure analysis software for powder diffraction data. User's Manual. Karlsruhe, Germany: Bruker AXS.
25. Cheary RW, Coelho AA. A fundamental parameters approach to X-ray line-profile fitting. *J Appl Crystallogr* 1992;**25**:109–21.
26. Young RA. In: Young RA, editor. *Introduction to the Rietveld method—the Rietveld method, IUCr Book Series*. Oxford University Press; 1993. p. 1–39.
27. CIE. Recommendations on uniform colour spaces, colour difference equations, psychometrics colour terms. In Suplement no. 2 of CIE Publ. No. 15 (E1-1.31) 1971, Paris: Bureau Central de la CIE; 1978.
28. ICSD. Inorganic crystal structure database, developed by FIZ Karlsruhe (The new ICSD Web is available from June 2009 at http://icsd.fiz-karlsruhe.de/icsd).
29. Shannon RD. Revised effective ionic radii and systematic studies of interatomic distances in halides and chalcogenides. *Acta Crystallogr* 1976;**A32**:751–67.
30. El Bali B, Bolte M. Refinement of cobalt diphosphate against new intensity data. *Acta Crystallogr* 2002;**E58**:i32–3.
31. Nord AG, Stefanidis T. Structure refinements of $Co_3(PO_4)_2$. A note on the reliability of powder diffraction studies. *Acta Chem Scand A* 1983;**37**:715–21.
32. Lever ABP. *Inorganic electronic spectroscopy*. second ed. The Netherlands: Elsevier Science B.V.; 1977. pp. 507–11.